Analysis of Spherical-Rectangular Microstrip Antennas

L. A. Costa, O. M. C. Pereira-Filho e F. J. S. Moreira

Department of Electronic Engineering - Federal Univ. of Minas Gerais

***Abstract*— The radiation pattern of spherical-rectangular microstrip antennas is investigated using the Cavity Method and the Electric Surface Current Method. The thickness of the dielectric substrate and its relative permittivity are varied and the effects on the radiation pattern are analyzed.**

***Index Terms*— Microstrip antennas on spherical surfaces, Cavity method, Electric surface current method.**

I. Introduction

Microstrip antennas have been widely used due to their low cost, low weight and ability to integrate with microwave circuits. They are specially important in several applications, like on aircrafts, where the antenna is required to conform to their external surfaces.

Spherical microstrip antennas have been analyzed using a variety of methods. The cavity method [1] was used in [2] to analyze circular disks, wraparound, and annular ring antennas. The electrical surface current method [3] was used in [4], when studying a circular disk. While in [5] an uniform magnetic surface current was used for modeling a wraparound antenna. The method of moments [6] has also been applied to spherical microstrip antennas. In [7] the resonances of a circular disk were determined using Galerkin's procedure with basis functions obtained from the cavity model. While [8] studied the effects of a superstrate on the properties of the circular disk.

All the previously mentioned works dealt with symmetric structures to the polar axis of the mounting sphere, i.e, circular disks, wraparound and annular ring antennas. Spherical-rectangular antennas were first studied in [9] using cavity method, but in this case the image theory was also applied, as if in the presence of an infinite ground plane. As a consequence the results are inaccurate for the back-lobes and when the sphere radius diminishes. In [10] and [11] spherical-rectangular microstrip antennas were analyzed using the electric surface current method. However it was assumed that the patch was centered on the x-y plane, having parallel sides. Arrays were formed by displacing this patch, maintaining its shape. Furthermore the electric current was assumed sinusoidal, which is only appropriate for an almost planar antenna.

In the present paper, we analyze a spherical-rectangular microstrip antenna, as shown in Fig. 1, using both the cavity and the electric surface current methods. The cavity method is limited to analyses where the dielectric thickness is much smaller than the radius of the mounting sphere and the wavelength in the dielectric, to assure that the fields are almost completely confined in the substrate between the metallic patch and the ground. On the other hand the fields obtained with the electric surface current method take into account the dielectric layer and are sensitive to the changes in the dielectric thickness. Other than [9], the radiation patterns obtained here are accurate in the entire region around the mounting sphere, not only in the front-lobe. Furthermore the patch can be centered at any point in the sphere, and the electric current distribution used in the electric surface current method is obtained from the cavity method, which will prove to be more accurate than that used in [10]. Comparison and limitations of the methods are discussed.

II. Theoretical Formulation

The geometry of the spherical-rectangular microstrip antenna is shown in Fig. 1. A perfect electric conducting sphere with radius r_1 is covered by a dielectric layer with thickness δr and relative permittivity ϵ_r. A patch of perfect electric conductor is placed on the dielectric layer, limited by the angles θ_1 and θ_2 ($\theta_2 = \theta_1 + \delta\theta$), and by ϕ_1 and ϕ_2 ($\phi_2 = \phi_1 + \delta\phi$), in spherical coordinates.

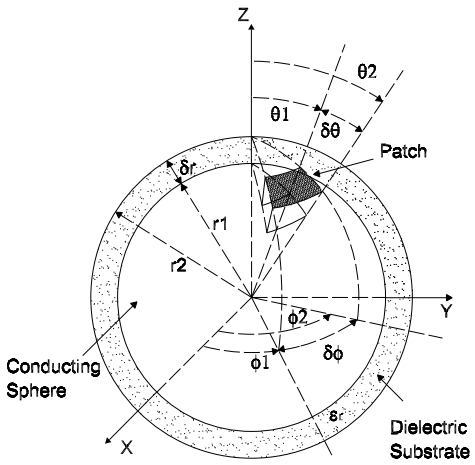

Fig. 1. Geometry of Spherical-rectangular Microstrip Antenna

A. Cavity Method

The cavity method is widely used in microstrip antenna problems. It is based on the fact that the field remains almost totally confined under the patch, configuring a cavity that has perfect electric top and bottom walls and perfect magnetic side walls. For each resonance mode of the cavity, the equivalent magnetic currents on the side walls are determined and considered to radiate in presence of the conducting sphere but without the dielectric layer. This assumption have been shown satisfactory for a very thin dielectric layer.

It is known that the TE_r cavity modes radiate poorly, as the corresponding equivalent magnetic currents are always normal to the surface of the conducting sphere. For the TM_r modes, only the radial component of the electric field, $E_r^{cav}\hat{r}$, can produce equivalent magnetic currents, which effectively radiate.

The radial component of the magnetic vector potential is a solution of [12]:

$$(\nabla^2 + k_d^2)\frac{A_r^{cav}}{r} = 0 \tag{1}$$

where $k_d = w\sqrt{\mu_o \epsilon_o \epsilon_r}$.

Applying the method of separation of variables and enforcing the boundary conditions, the radial component of the magnetic vector potential is given by:

$$\begin{aligned} A_r^{cav} = & -k_d \sin(\theta_1) \\ & \times[\hat{N}'_{\nu_r}(k_d r_1)\hat{J}_{\nu_r}(k_d r) - \hat{J}'_{\nu_r}(k_d r_1)\hat{N}_{\nu_r}(k_d r)] \\ & \times[Q_{\nu_r}^{\mu_r\prime}(\cos(\theta_1))P_{\nu_r}^{\mu_r}(\cos(\theta)) \\ & - P_{\nu_r}^{\mu_r\prime}(\cos(\theta_1))Q_{\nu_r}^{\mu_r}(\cos(\theta))] \\ & \times \cos(\mu_r[\phi - \phi_1]) \end{aligned} \tag{2}$$

where $\hat{J}_\nu(x)$, $\hat{N}_\nu(x)$, and $\hat{H}_\nu^{(2)}(x)$ are the Schelkunoff type Bessel, Neumann, and second-kind Hankel functions, respectively. The functions $P_\nu^\mu(x)$ and $Q_\nu^\mu(x)$ are the Associated Legendre functions of first and second kind, respectively. The parameters μ_r, ν_r and k_d are solutions of the transcendental equations that determine the resonant modes inside the cavity:

$$\mu_r = \frac{m\pi}{\Delta\phi} \qquad m = 0, 1, 2, 3, \ldots \tag{3}$$

$$\begin{aligned} & Q_{\nu_r}^{\mu_r\prime}(\cos(\theta_1))P_{\nu_r}^{\mu_r\prime}(\cos(\theta_2)) \\ & \qquad = P_{\nu_r}^{\mu_r\prime}(\cos(\theta_1))Q_{\nu_r}^{\mu_r\prime}(\cos(\theta_2)) \end{aligned} \tag{4}$$

$$\hat{N}'_{\nu_r}(k_d r_1)\hat{J}'_{\nu_r}(k_d r_2) = \hat{J}'_{\nu_r}(k_d r_1)\hat{N}'_{\nu_r}(k_d r_2) \tag{5}$$

The radial component of the electric field is then given by:

$$\begin{aligned} E_r^{cav} = & j\eta_d \frac{\nu_r(\nu_r+1)}{r^2}\sin(\theta_1) \\ & \times[\hat{N}'_{\nu_r}(k_d r_1)\hat{J}_{\nu_r}(k_d r) - \hat{J}'_{\nu_r}(k_d r_1)\hat{N}_{\nu_r}(k_d r)] \\ & \times[Q_{\nu_r}^{\mu_r\prime}(\cos(\theta_1))P_{\nu_r}^{\mu_r}(\cos(\theta)) \\ & - P_{\nu_r}^{\mu_r\prime}(\cos(\theta_1))Q_{\nu_r}^{\mu_r}(\cos(\theta))] \\ & \times \cos(\mu_r[\phi - \phi_1]) \end{aligned} \tag{6}$$

where η_d is the dielectric intrinsic impedance.

The equivalent magnetic current, which is superficial, can be transformed into filamentary current due to the low thickness of the dielectric layer. In that way, $\vec{M}_{eq}$ is filamentary and given by:

$$\vec{M}_{eq} = -\int_{r_1}^{r_2} \vec{n} \times \vec{E}^{cav}\Big|_{\text{side walls}}\, dr \tag{7}$$

where $\vec{n}$ is directed outward from the cavity.

The radiation fields due to M_{eq} are obtained without considering the presence of the dielectric, through the radial components of vector potentials:

$$A_r^o = \sum_{n=1}^{+\infty}\sum_{m=-n}^{+n} e_{mn}\hat{H}_n^{(2)}(k_o r)P_n^{|m|}(\cos(\theta))e^{jm\phi} \tag{8}$$

$$F_r^o = \sum_{n=1}^{+\infty}\sum_{m=-n}^{+n} f_{mn}\hat{H}_n^{(2)}(k_o r)P_n^{|m|}(\cos(\theta))e^{jm\phi} \tag{9}$$

The coefficients e_{mn} and f_{mn} are determined by the boundary conditions of the electromagnetic fields on the conducting sphere surface, which is most easily accomplished in the domain of the Fourier-Legendre vectorial transform [4], [7].

B. Electric Surface Current Method

The surface currents method calculates the radiated field from the knowledge of the induced electric currents on the patch. Other than the cavity method, the electric surface current method takes into account the dielectric layer through the proper Green's Functions. A good approximation for those currents is obtained from the magnetic field of the cavity theory. Once again it can be considered that only TM_r modes exist inside the cavity, which magnetic field is given by:

$$\begin{aligned} H_\theta^{cav} = & \frac{k_d \mu_r \sin(\theta_1)}{r\sin(\theta)} \\ & \times[\hat{N}'_{\nu_r}(k_d r_1)\hat{J}_{\nu_r}(k_d r) - \hat{J}'_{\nu_r}(k_d r_1)\hat{N}_{\nu_r}(k_d r)] \\ & \times[Q_{\nu_r}^{\mu_r\prime}(\cos(\theta_1))P_{\nu_r}^{\mu_r}(\cos(\theta)) \\ & - P_{\nu_r}^{\mu_r\prime}(\cos(\theta_1))Q_{\nu_r}^{\mu_r}(\cos(\theta))] \\ & \times \sin(\mu_r[\phi - \phi_1]) \end{aligned} \tag{10}$$

$$H_{\phi}^{cav} = \frac{-k_d \sin(\theta_1)\sin(\theta)}{r} \times[\hat{N}'_{\nu_r}(k_d r_1)\hat{J}_{\nu_r}(k_d r) - \hat{J}'_{\nu_r}(k_d r_1)\hat{N}_{\nu_r}(k_d r)] \times[Q_{\nu_r}^{\mu_r\prime}(\cos(\theta_1))P_{\nu_r}^{\mu_r\prime}(\cos(\theta)) - P_{\nu_r}^{\mu_r\prime}(\cos(\theta_1))Q_{\nu_r}^{\mu_r\prime}(\cos(\theta))] \times \cos(\mu_r[\phi - \phi_1]) \quad (11)$$

The induced currents are:

$$\vec{J}_{ind}^{patch} = -\hat{r} \times \vec{H}^{cav}\Big|_{\text{top wall}} \quad (12)$$

The induced electric currents are the source of the radiation field which can be expanded in TM_r and TE_r modes. The vector potentials in the free-space have the same form as in (8) e (9), however in the dielectric layer, they are given by:

$$A_r^d = \sum_{n=1}^{+\infty}\sum_{m=-n}^{+n}\{a_{mn}[\hat{J}_n(k_d r) + b_{mn}\hat{N}_n(k_d r)] \times P_n^{|m|}(\cos(\theta))e^{jm\phi}\} \quad (13)$$

$$F_r^d = \sum_{n=1}^{+\infty}\sum_{m=-n}^{+n}\{c_{mn}[\hat{J}_n(k_d r) + d_{mn}\hat{N}_n(k_d r)] \times P_n^{|m|}(\cos(\theta))e^{jm\phi}\} \quad (14)$$

The coefficients a_{mn}, b_{mn}, c_{mn}, d_{mn}, e_{mn} e f_{mn} are determined enforcing the boundary conditions of the electromagnetic fields on the surfaces of the dielectric layer. Once again, the matching of the boundary conditions is most easily accomplished in the domain of the Fourier-Legendre vectorial transform, [4], [7].

III. Results

Initially the results from both formulations are compared with those from [13], using method of moments, for a spherical circular antenna. The radiation pattern is shown in Fig. 2 in the E-plane, with the present formulations operating in the TM_{10} mode, and a very good match is observed.

Figure 3 compares the radiation pattern obtained with the present formulations, operating in TM_{01} mode, with that from [10], for a spherical-rectangular patch centered at the x-y plane. It is observed that the cavity model and the present electric surface current model provide very similar results, while that from [10] shows a higher back-lobe. It is a consequence of the θ-variation of the currents, obtained here from the associate Legendre functions, solution of the wave equation, in comparison with a simpler sinusoidal variation assumed in [10].

Figure 4 and 5 show the radiation patterns of a spherical-rectangular antenna as a function of the dielectric thickness

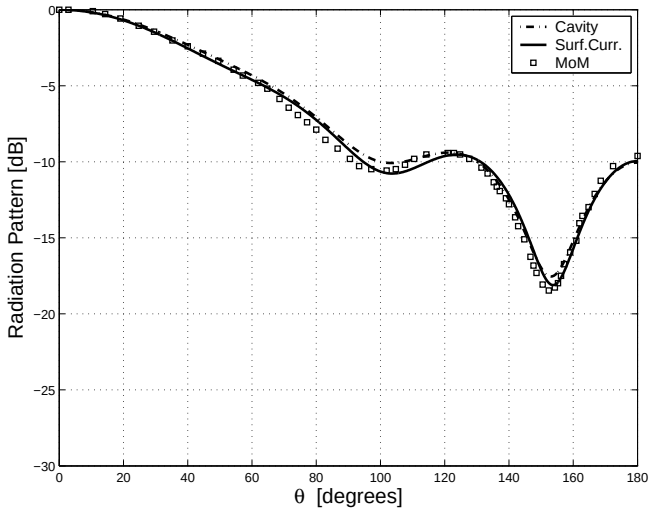

Fig. 2. E-plane Radiation Pattern of spherical circular antenna: $\epsilon_r = 2.47$, $\delta\phi = 2\pi$, $r_1 = 5$ cm, $\delta_r = 0.16$ cm, $\theta_1 \approx 0$, $r_1\theta_2 = 1.88$ cm, f=2.96 GHz.

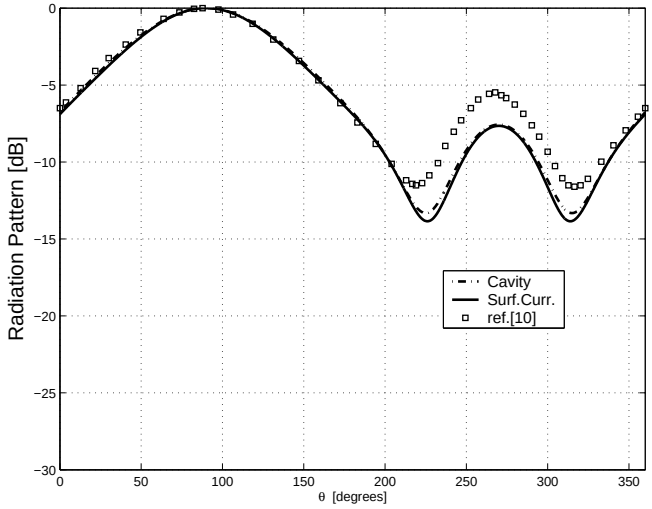

Fig. 3. Radiation Pattern on E-plane for a spherical-rectangular patch of sides 4.8 x 4.8 cm, centered at $\theta = \pi/2$, $r_1 = 0.25\lambda_o$, $\epsilon_r = 2.32$, $\delta_r = 1.58$ mm, f=2 GHz.

and dielectric constant, respectively. The constant dimensions are : $r_1 = 20$ cm, $\theta_1 = 25^{\text{o}}$, $\delta\theta = 10^{\text{o}}$, $\phi_1 = 60^{\text{o}}$ and $\delta\phi = 60^{\text{o}}$. It is convenient to note that all the dimensions already consider the fringing fields [14]. In Fig. 4 the relative permittivity is kept constant $\epsilon_r = 4.4$, while the thickness varies from 1 to 10 mm, obtaining 0.683 GHz and 0.668 GHz as their fundamental resonance frequencies respectively. It is observed that while the results from cavity method are unchanged, as expected, those from electric surface current method show an increase in the back-lobes due to the excitation of surface waves. In

the Fig. 5 the dielectric thickness which is kept constant ($\delta_r = 1$ mm) while the relative permittivity varies from 1.06 to 3.76, obtaining 1.391 GHz and 0.739 GHz as their fundamental resonance frequencies respectively. In this case both methods show an increase in the back-lobe, due to the surface waves.

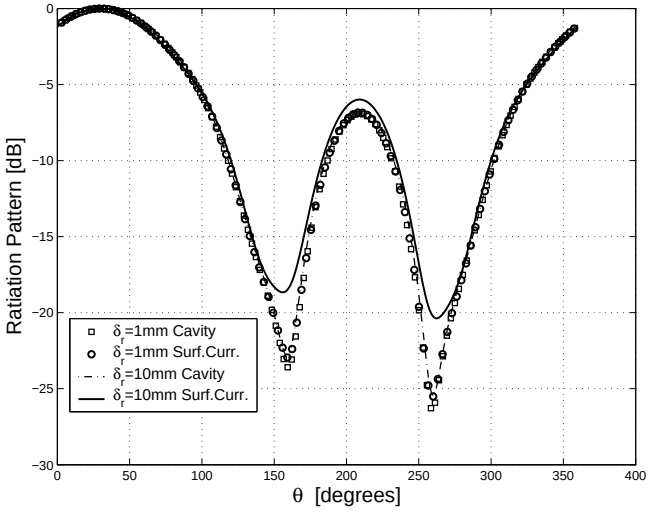

Fig. 4. Radiation pattern of a spherical-rectangular antenna (z-y plane): $r_1 = 20$ cm, $\theta_1 = 25^o$, $\delta\theta = 10^o$, $\phi_1 = 60^o$, $\delta\phi = 60^o$, $\epsilon_r = 4.4$.

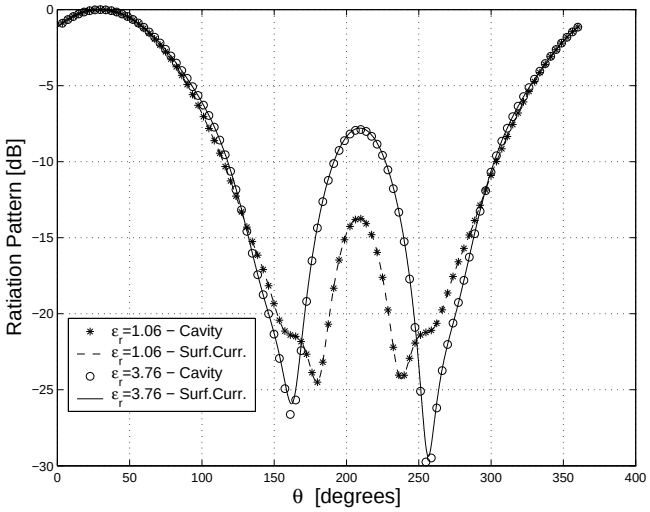

Fig. 5. Radiation pattern of a spherical-rectangular antenna (z-y plane): $r_1 = 20$ cm, $\theta_1 = 25^o$, $\delta\theta = 10^o$, $\phi_1 = 60^o$, $\delta\phi = 60^o$, $\delta_r = 1$ mm.

IV. Conclusion

This paper presented two procedures for analyzing spherical-rectangular microstrip antennas, i.e., cavity method and electric surface current method. It shows the radiation pattern of such antenna positioned at any point on the sphere, and the effects of variations of dielectric constant e thickness.

References

[1] Y.T.Lo, D.Soloman and W.F.Richards, "Theory and experiment on microstrip antennas", IEE Trans.,1979, AP-27, pp.137-145.

[2] W.Y.Tam and K.M.Luk, "Patch antennas on a Spherical Body", IEEE Proc.-H. vol. 138, No.1,February 1991, pp. 103-108.

[3] J.Ashkenazy, S.Shtrikman and D. Treves, "Electric surface current model for the analysis of microstrip antennas an cylindrical bodies", IEE Trans.,1985, AP-33, pp.295-300.

[4] W.Y.Tam and K.M.Luk, "Far field analysis of spherical-circular microstrip antennas by electric surface current models", IEEE Proc.-H. vol. 138, No.1,February 1991, pp. 98-102.

[5] A. Das, S.K. Das and M.S. Narasimhan, "Resonance Characteristics of Wraparound Microstrip Antenna on Spherical Body", IEEE Trans. Antennas Propagat., vol. 39, pp. 1031-1034, July. 1991.

[6] R.F.Harrington, "Field Computation by Moment Method", Macmillian, New York, 1968.

[7] W.Y.Tam and K.M.Luk, "Resonance in Spherical-Circular Microstrip Structures", IEEE Trans. Microwave Theory Tech. vol. 39, No.4,April 1991, pp. 700-704.

[8] K.L. Wong, S.F. Hsiao and H.T. Chen, "Resonance and Radiation of a Supestrate-Loaded Spherical-Circular Microstrip Patch Antenna", IEEE Trans. Antennas Propagat., vol. 41, pp. 686-690, May. 1993.

[9] K.Y.Wu and J.F.Kauffman, "Radiation Pattern for Spherical-Rectangular Microstrip Antennas", IEEE Antennas Propagat. Int. Symposium Digest, 1983, pp. 43-46.

[10] N.Burum and Z.Sipus, "Radiation Pattern of Spherical Array of Rectangular Microstrip Patches", Proc. of IEEE Int. Symposium on Antennas and Propagation, SanAntonio,USA, 2002, pp.96-99.

[11] N.Burum, S. Rupcic and Z.Sipus, "Theoretical and Experimental Study of Spherical Arrays", Procedings of IEEE MELECON 2004, Dubrovnik, Croatia, pp. 503-06.

[12] R.F.Harrington, "Time harmonic electromagnetic fields", McGraw-Hill, New York, 1961.

[13] B.Ke and A.A.Kishk, "Analysis of spherical circular microstrip Antennas", IEEE Proc.-H. vol. 138, No.6 , Dec. 1991, pp. 542-548.

[14] E.Chang, S.A.Long and W.F.Richards, "An Experimental Investigation of Electrically Thick rectangular Microstrip Antennas", IEEE Trans. Antennas Propagat., vol. AP-34, No.6 ,June 1986, pp. 767-772.